

Title	Ultra-low-dose thoracic CT with model-based iterative reconstruction (MBIR) in cystic fibrosis patients undergoing treatment with cystic fibrosis transmembrane conductance regulators (CFTR)
Authors	Moloney, Fiachra;Kavanagh, Richard G.;Ronan, Nicola J.;Grey, T. M.;Joyce, Stella;Ryan, David J.;Moore, Niamh;O'Connor, Owen J.;Plant, Barry J.;Maher, Michael M.
Publication date	2021-01-16
Original Citation	Moloney, F., Kavanagh, R.G., Ronan, N.J., Grey, T. M., Joyce, S., Ryan, D.J., Moore, N., O'Connor, O.J., Plant, B. J. and Maher, M. M. (2021) 'Ultra-low-dose thoracic CT with model-based iterative reconstruction (MBIR) in cystic fibrosis patients undergoing treatment with cystic fibrosis transmembrane conductance regulators (CFTR)', Clinical Radiology, 76(5), pp. 393.e9 - 393.e17. doi: 10.1016/j.crad.2020.12.003
Type of publication	Article (peer-reviewed)
Link to publisher's version	10.1016/j.crad.2020.12.003
Rights	© 2021, the Authors. Published by Elsevier Ltd on behalf of The Royal College of Radiologists. This is an open access article under the CC BY license. - <a href="https://creativecommons.org/licenses/by/4.0/">https://creativecommons.org/licenses/by/4.0/</a>
Download date	2023-05-05 08:38:44
Item downloaded from	<a href="http://hdl.handle.net/10468/12049">http://hdl.handle.net/10468/12049</a>



# Ultra-low-dose thoracic CT with model-based iterative reconstruction (MBIR) in cystic fibrosis patients undergoing treatment with cystic fibrosis transmembrane conductance regulators (CFTR)

F. Moloney<sup>a,b</sup>, R.G. Kavanagh<sup>a,b</sup>, N.J. Ronan<sup>c,d</sup>, T.M. Grey<sup>b</sup>, S. Joyce<sup>b,\*</sup>, D.J. Ryan<sup>a,b</sup>, N. Moore<sup>e</sup>, O.J. O'Connor<sup>a,b,f</sup>, B.J. Plant<sup>c,d</sup>, M.M. Maher<sup>a,b,f</sup>

<sup>a</sup> Department of Radiology, Cork University Hospital, Wilton, Cork, Ireland

<sup>b</sup> Department of Radiology, School of Medicine, University College Cork, Ireland

<sup>c</sup> Cork Cystic Fibrosis Centre, Cork University Hospital, Wilton, Cork, Ireland

<sup>d</sup> HRB Clinical Research Facility, Cork University Hospital, University College Cork, Ireland

<sup>e</sup> Department of Radiography, University College Cork, Ireland

<sup>f</sup> APC Microbiome, University College Cork, Ireland

## ARTICLE INFORMATION

### Article history:

Received 9 July 2020

Accepted 11 December 2020

**AIM:** To assess the utility of a volumetric low-dose computed tomography (CT) thorax (LDCTT) protocol at a dose equivalent to a posteroanterior (PA) and lateral chest radiograph for surveillance of cystic fibrosis (CF) patients.

**MATERIALS AND METHODS:** A prospective study was undertaken of 19 adult patients with CF that proceeded to LDCTT at 12 and 24 months following initiation of ivacaftor. A previously validated seven-section, low-dose axial CT protocol was used for the 12-month study. A volumetric LDCTT protocol was developed for the 24-month study and reconstructed with hybrid iterative reconstruction (LD-ASIR) and pure iterative reconstruction (model-based IR [LD-MBIR]). Radiation dose was recorded for each scan. Image quality was assessed quantitatively and qualitatively, and disease severity was assessed using a modified Bhalla score. Statistical analysis was performed and *p*-values of <0.05 were considered statistically significant.

**RESULTS:** Volumetric LD-MBIR studies were acquired at a lower radiation dose than the seven-section studies ( $0.08 \pm 0.01$  versus  $0.10 \pm 0.02$  mSv;  $p=0.02$ ). LD-MBIR and seven-section ASIR images had significantly lower levels of image noise compared with LD-ASIR images ( $p<0.0001$ ). Diagnostic acceptability scores and depiction of bronchovascular structures were found to be acceptable for axial and coronal LD-MBIR images. LD-MBIR images were superior to LD-ASIR images for all qualitative parameters assessed ( $p<0.0001$ ). No significant change was observed in mean Bhalla score between 1-year and 2-year studies ( $p=0.84$ ).

\* Guarantor and correspondent: S. Joyce, Department of Radiology, University College Cork, Cork University Hospital, Wilton, Cork, Ireland. Tel.: +00353868340492.

E-mail address: [stella.joyce@umail.ucc.ie](mailto:stella.joyce@umail.ucc.ie) (S. Joyce).

**CONCLUSIONS:** The use of a volumetric LDCTT protocol (reconstructed with pure IR) enabled acquisition of diagnostic quality CT images, which were considered extremely useful for surveillance of CF patients, at a dose equivalent to a PA and lateral chest radiograph.

© 2021 The Authors. Published by Elsevier Ltd on behalf of The Royal College of Radiologists. This is an open access article under the CC BY license (<http://creativecommons.org/licenses/by/4.0/>).

## Introduction

Pulmonary disease is the primary cause of morbidity and mortality in patients with cystic fibrosis (CF).<sup>1</sup> Early detection of the onset of lung disease and complications is essential to facilitate expedient treatment adaptation with the ultimate aim of limiting disease progression.<sup>2</sup> The current annual rate of lung function decline (FEV<sub>1</sub>) among all patients with CF is approximately 0.7%, making it difficult to detect subtle changes with standard monitoring methods, such as chest radiography and pulmonary function tests (PFTs).<sup>3</sup> Several studies have demonstrated computed tomography (CT) to be more sensitive than chest radiography and PFTs for the detection and surveillance of lung disease,<sup>4,5</sup> potentially making it the most appropriate technique for monitoring pulmonary disease in the current CF population.

The major limitation to routine adoption of CT for monitoring CF lung disease is the substantial radiation exposure associated with conventional chest CT compared with plain radiography (3.5 versus 0.02 mSv).

Several dose optimisation strategies may be employed when performing chest CT in patients with CF; the use of low-dose protocols may include automated exposure control, and automated patient centring techniques.<sup>6</sup> At Cork Cystic Fibrosis Centre, Cork University Hospital, a specialised CF centre, a previously published seven-section low-dose protocol is used, consisting of a limited number of thin CT sections to impart a mean effective dose of 0.14mSv, equivalent to the dose of a posteroanterior (PA) and lateral chest radiograph.<sup>7</sup> The unit has used this protocol on a routine basis to monitor pulmonary disease in CF patients in a study assessing the safety, efficacy, and tolerability of a range of CF transmembrane conductance regulator (CFTR) drugs including ivacaftor (Kalydeco).<sup>8</sup> Ivacaftor has been shown to produce significant increases in forced expiratory volume in 1 second (FEV<sub>1</sub>) (>10% absolute) and body mass index (BMI), as well as reductions in sweat chloride levels, patient-reported respiratory symptoms, and pulmonary exacerbation rate in patients with the G551D-CFTR mutation.<sup>9–11</sup> The prevalence of this Class III gating mutation, known as the Celtic mutation<sup>12</sup> at Cork Cystic Fibrosis Centre is the highest in the world at 23%,<sup>8</sup> compared with 4% in the United States,<sup>13</sup> making it uniquely placed to provide single-centre insight into CFTR potentiation. CFTR mutation frequencies are highly variable and demonstrate regional differences in prevalence.<sup>14,15</sup> This heterogeneity is thought to be explained by the ethnic or geographic origin of the parents and grandparents of the affected child.<sup>14</sup>

The efficacy of many dose reduction strategies in CT was often limited by the restraints of traditional filtered back projection (FBP) reconstruction algorithms installed on most CT systems. Iterative reconstruction (IR) algorithms, which incorporate statistical information of the CT system, including photon statistics and electronic acquisition noise, have been the focus of much dose optimisation research in recent years. Although available on early CT scanners, IR was not clinically useful as the necessary computing power was not widely available. With modern advances in computer technology, IR has now become a viable option to achieve significant dose reductions. Hybrid IR algorithms, such as adaptive statistical IR (ASIR - GE Healthcare, Milwaukee, WI, USA) are the most studied methods to date in chest CT, facilitating dose reductions of the order of 57% while preserving image quality.<sup>16,17</sup> In recent years, a more computationally intense pure IR algorithm, which includes model-based IR (MBIR); Veo (GE Healthcare, GE Medical Systems), that uses a more complex system of prediction models has become commercially available. As each manufacturer has their own vendor-specific IR algorithms, which are now widely available, the implementation of low-dose CT protocols should be achievable in all centres.<sup>18</sup> To date, there is a paucity of studies assessing the use of pure IR in chest CT.<sup>19</sup>

The purpose of this prospective feasibility study was to assess the feasibility of replacing a standard chest radiograph with a similar dose volumetric low-dose protocol CT thorax (LDCTT), reconstructed with pure IR, for the surveillance of pulmonary disease in patients with CF.

## Materials and methods

### Study population

Institutional review board approval was granted for this study. This study forms part of a prospective study conducted at Cork Cystic Fibrosis Centre, a designated tertiary CF centre, assessing the impact of the CF transmembrane conductance regulator, ivacaftor on the CF lung.<sup>8</sup> As part of this study, between March 2014 and January 2016, 19 (nine male (47%), 10 female) clinically stable, ivacaftor-naïve adult patients with CF and at least one copy of the G551D allele gave written informed consent to undergo a low-dose CT thorax prior to ivacaftor treatment followed by radiological follow-up with low-dose CT thorax at 12 and 24 months. Overall, mean age at the 12 month CT was 29.5 ± 10.5 years (males: 25.6 ± 7.4 and females: 33.9 ± 12.1 years;  $p=0.08$ ).

### CT technique and image reconstruction

All studies were acquired using a 64-section multi-detector CT system (Discovery CT 750 HD; GE Healthcare, GE Medical Systems) without intravenous contrast material.

#### Seven-section low-dose protocol

A previously validated, modified seven-section, low-dose axial CT protocol was used for the pre-treatment and first 12-month studies.<sup>7</sup> Single anteroposterior and mediolateral localiser radiographs were used to identify five levels at which images were acquired (Fig 1). Images were obtained at end-inspiration through the apices, aortopulmonary window, carina, and at widest cardiac and thoracic diameters (Fig 2a–e). A further two images were obtained with the patient in full expiration at the level of the aortopulmonary window and widest cardiac diameter (Fig 2f). The following parameters were used: 120 kV tube voltage, 0.4 seconds gantry rotation time, 32 cm field of view (FOV), and z-axis automatic tube current modulation with minimum and maximum tube current thresholds of 10 and 100 mA with noise index of 29 HU. Images were acquired at each level at section thickness of 0.625 mm and reconstructed to a section thickness of 3 mm, employing hybrid IR of 40% ASIR and 60% filtered back projection, labelled seven-section ASIR.

#### Volumetric low-dose protocol

A novel low-dose volumetric protocol was designed for 24-month surveillance CT. Preliminary anthropomorphic torso phantom (CT Torso Phantom CTU41, Kyoto Kagaku, Fushimi-ku, Kyoto, Japan) and technical phantom (Catphan 600, The Phantom Laboratory, Greenwich, NY, USA) studies were conducted to determine the optimal protocol settings. Technical parameters were altered to assess radiation dose and diagnostic quality with the following parameters indicating that studies could potentially be acquired at a dose of approximately 0.08mSv: 80 kV tube voltage, 20mA tube

current, 0.4 seconds gantry rotation time, 1.375 pitch factor, and FOV of 32 cm. To ensure radiation exposure remained low for all patients, a fixed tube current technique was employed. Scanning was performed at end-inspiration from lung apices to bases, including costophrenic recesses. In the interests of minimising radiation exposure, no additional expiratory phase imaging was performed. Images were acquired at section thickness of 0.625mm and reconstructed at final section thickness of 3 mm with pure IR (MBIR) in axial, coronal, and sagittal planes (labelled LD-MBIR; Fig 3). Images were also reconstructed with hybrid IR (40% ASIR and 60% filtered back projection), labelled LD-ASIR. Images were further reconstructed at the same five levels as seven-section ASIR inspiratory phase scans to facilitate a direct, blinded comparison between both low-dose techniques.

#### Dose measurements

Dose–length product (DLP) and volume CT dose index (CTDIvol) values were recorded from each CT dose report. Calibration of CT unit was performed once per week in accordance with manufacturer's instructions and following the departmental quality-assurance protocol. The Imaging Performance and Assessment in CT patient dosimetry calculator (ImpACT version 0.99x, London, UK) was used to calculate the effective dose (ED). The radiation exposure resultant from the CT topograms was excluded from analysis, following methodology of previous published studies, and justified by negligible radiation exposures associated with CT topograms.

#### Quantitative analysis

Objective image quality analysis was performed independently on a dedicated workstation (Advantage Workstation VolumeShare 2, Version 4.4, GE Medical Systems) by two operators with 6 and 7 years of radiology experience, respectively. The operators were blinded to imaging protocol and the order of the datasets was randomised. Attenuation values were measured in Hounsfield units at three levels: the aortic arch, the carina, and maximum cardiac diameter. Measurements were recorded by placing circular regions of interest (ROIs) of equal size (10 mm diameter) in the descending aorta and paraspinal muscles of posterior chest wall at each level. The ROIs were placed in as homogeneous an area as possible, taking care to avoid fat planes and blood vessels. The standard deviation of the attenuation in ROI served as an objective measure of image noise. The SNR of each ROI was calculated by dividing the mean attenuation by its standard deviation. Measurements were taken three times by each operator to minimise error. The mean of both operators' measurements was used for analysis.

#### Qualitative analysis

The 24-month LD-MBIR images were compared with the same data reconstructed using ASIR (LD-ASIR). Digital images were reviewed on a PACS (Impax 6.5.3; Agfa Healthcare, Morstel, Belgium) on a monitor with resolution of 3

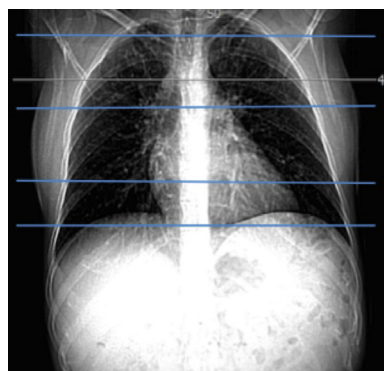


**Figure 1** Anteroposterior scanned projection radiograph used to identify five levels at which images were acquired for the seven-section low-dose protocol. Images were obtained at the level of the lung apices, aortopulmonary window, carina, and at the widest cardiac and thoracic diameters.



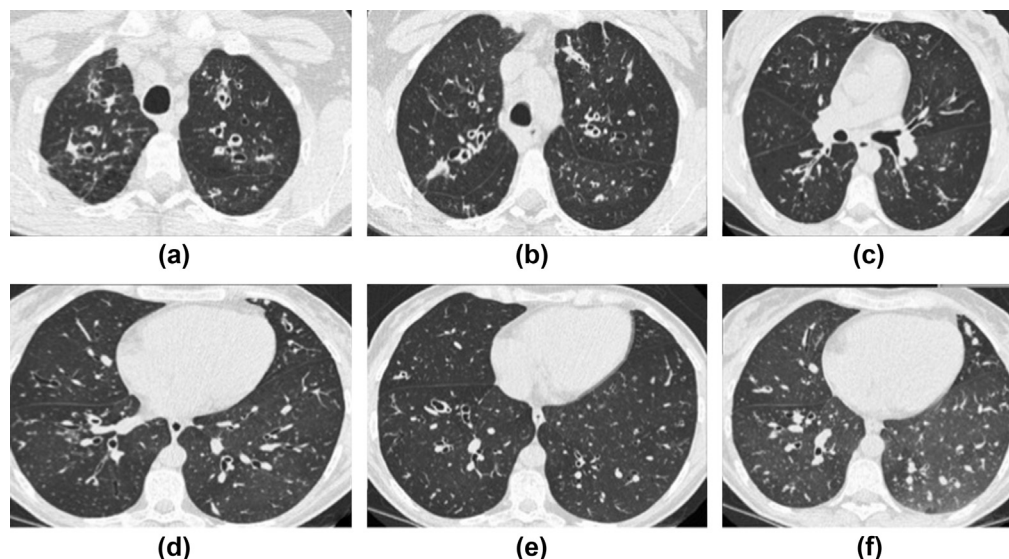


**Figure 2** Low-dose axial CT images acquired in a 21-year-old man with CF at 12-months of treatment with ivacaftor using the seven-section ASIR protocol (effective dose 0.1 mSv). Images were obtained at the level of the lung apices (a), aortopulmonary window (b), carina (c), and at the widest cardiac (d) and thoracic (e) diameters. Expiration phase images were obtained at the level of the aortopulmonary window (not shown) and at the widest cardiac diameter (f).



**Figure 3** Representative coronal CT image acquired in a 23-year-old man with CF at 24 months of treatment with ivacaftor using the volumetric low-dose pure IR protocol (effective dose 0.08 mSv).

megapixels. Image noise, diagnostic acceptability, depiction of bronchovascular structures within 2 cm of the pleural margin, and presence of streak artefact were assessed in consensus by two radiologists, with 13- and 22-years radiology experience, respectively, at the five anatomical levels for all datasets. The subjective image quality parameters and grading system were selected and assessed as in prior studies.<sup>7</sup>

#### Quantification of lung disease

Disease severity was scored independently by the same two radiologists (who had significant prior experience of assessing severity of CF) using Bhalla system.<sup>20</sup> To minimise the effects of recall bias, all datasets were anonymised and reviewed in a random order. In addition, a 6-week delay was instituted between review of the 12

month seven-section ASIR studies and the 24-month LD-MBIR studies. Images were reviewed on lung window settings (1500 HU window width, –500 HU window level) on a PACS system using axial reformations for seven-section ASIR studies and a combination of axial and coronal reformations for LD-MBIR studies.

The presence and severity of nine morphological changes were evaluated including: severity of bronchiectasis; peribronchial thickening; extent of bronchiectasis (number of bronchopulmonary segments); extent of mucus plugging (number of lung segments); abscesses or sacculations (number of lung segments); generations of the bronchial divisions involved; number of bullae; and collapse/consolidation following Bhalla system.<sup>20</sup> Assessment for air-trapping forms part of the assessment using the Bhalla scoring system, but this could not be assessed on the volumetric low-dose protocol (LDCT) as expiration scans were not performed. Therefore, a modified Bhalla score, excluding assessment for air trapping, was used for the 12 and 24-month CT examinations.

#### Statistical analysis

Data were exported from Microsoft Office Excel 2010 (Microsoft Corporation, Redmond, WA, USA) into GraphPad Prism version 7.1 (GraphPad Software Incorporated, San Diego, CA, USA) and Statistical Package for the Social Sciences (SPSS) version 22 (IBM, Chicago, IL, USA) for further analysis. Data are described as mean and standard deviation for parametric distributions or as median and range for non-parametric distributions. Mann–Whitney test was used to compare non-parametric distributions of two groups of continuous variables. Two-way analysis of variance and Tukey's multiple comparisons test were used to compare quantitative measures of noise and SNR.

Friedman's test was used to compare qualitative measures between datasets. Inter-rater reliability of disease quantification scores was assessed with intraclass correlations. Normally distributed repeated parametric quantitative indices were compared using paired *t*-tests. Pearson's correlations were used to assess the strength of association between normally distributed continuous variables. *p*-Values <0.05 were considered statistically significant.

## Results

### Radiation exposure

The 24-month volumetric LD-MBIR protocol was performed with a mean DLP of  $5.04 \pm 0.52$  mGy·cm corresponding to a mean ED of  $0.08 \pm 0.01$  mSv. The 12-month seven-section ASIR protocol was performed with a mean DLP of  $5.89 \pm 1.24$  mGy·cm with a mean ED of  $0.10 \pm 0.02$  mSv. LD-MBIR studies were acquired at a statistically significantly lower radiation dose than the seven-section ASIR studies (Table 1). The mean CTDIvol of the seven-section ASIR studies was significantly higher than the LD-MBIR studies as a much smaller volume of tissue received a similar radiation dose. Effective doses were reduced by 98.5% and 98.1% compared with conventional dose volumetric CT thorax in an adult patient (5.4 mSv) for the LD-MBIR and seven-section ASIR protocols, respectively.

### Quantitative analysis

Quantitative measures of image noise at three levels from each protocol are shown in Fig 4a. Both axial and coronal LD-MBIR images were significantly superior to LD-ASIR images at all levels (mean noise:  $23.03 \pm 6.4$  versus  $72.53 \pm 11.58$  HU ( $p < 0.0001$ ) and  $19.2 \pm 5.7$  versus  $72.53 \pm 11.58$  HU ( $p < 0.0001$ ), respectively). The greatest mean noise difference was observed between coronal LD-MBIR and LD-ASIR images, with the greatest difference at the level of maximum cardiac diameter (55.8 HU). All other comparisons at all levels were non-significant ( $p = 0.08$ – $0.94$ ). Seven-section ASIR images had significantly lower levels of image noise at all levels compared with LD-ASIR images ( $22.15 \pm 8.9$  versus  $72.53 \pm 11.58$  HU,  $p < 0.0001$ ).

Mean SNR was also compared between each protocol at each level (Fig 4b). Both axial and coronal LD-MBIR images had significantly higher SNRs than LD-ASIR images at all

levels ( $p < 0.001$  for all comparisons). Seven-section ASIR images also had significantly higher SNRs than LD-ASIR images at all levels ( $p < 0.0001$ ).

Coronal LD-MBIR images were found to have significantly higher SNRs than axial LD-MBIR images at the level of the maximum cardiac diameter ( $p = 0.0002$ ). Axial and coronal LD-MBIR images also had significantly higher SNRs than seven-section ASIR images at the level of the maximum cardiac diameter (*p*-values of 0.017 and 0.001, respectively). All other comparisons were non-significant.

### Qualitative analysis

No significant difference was found for five anatomical levels within each dataset for each parameter assessed; hence, the multilevel information was summated for comparison between protocols (Fig 5).

Axial and coronal LD-MBIR images were significantly superior to LD-ASIR images for all qualitative parameters assessed ( $p < 0.0001$  for all comparisons). Diagnostic acceptability scores on lung windows and depiction of bronchovascular structures within 2 cm of pleural margin were found to be acceptable for axial LD-MBIR images (median 3, range 1–4; median 3, range 1–5, respectively) and highly acceptable for coronal LD-MBIR images (median 4, range 2–5 for both) with coronal images being significantly superior ( $p < 0.0001$  for both comparisons). LD-ASIR images were minimally acceptable for both parameters (i.e., diagnostic acceptability scores on lung windows and depiction of bronchovascular structures; median 2, range 1–3 for both; Fig 6).

Streak artefact interfering with image interpretation was observed more often in the LD-ASIR images (median 3, range 2–3) than the LD-MBIR images ( $p < 0.0001$ ). Streak artefact was present on axial and coronal LD-MBIR images but it did not interfere with image interpretation (median 2, range 1–3 for both). No significant difference was observed in streak artefact between axial and coronal reformats. Streak artefact was greatest at the level of the lung apices for all reconstructions.

### Quantification of lung disease

Disease severity was assessed on 12-month seven-section ASIR studies and the 24-month LD-MBIR studies. Inter-rater variability measures were very good for total modified Bhalla score and all nine morphological changes for both the seven-section ASIR studies and the LD-MBIR studies, with intraclass correlations of 0.881 (95% confidence interval [CI]: 0.69 to 0.973,  $p < 0.001$ ) and 0.812 (95% CI: 0.439 to 0.937,  $p < 0.001$ ) for total modified Bhalla score, respectively; hence, mean reader scores were used to assess disease severity.

No significant change was observed in mean modified Bhalla score between 12-month and 24-month studies ( $11.03 \pm 2.7$  versus  $10.9 \pm 3.99$ ,  $p = 0.84$ ). There was moderate strength of association between modified Bhalla score and FEV<sub>1</sub> at 12 months ( $r = 0.43$ ,  $p = 0.1$ ) and 24 months ( $r = 0.78$ ,  $p = 0.01$ ). Bronchiectasis was the most severe and

**Table 1**  
Radiation dose metrics.

Dose measurement	Seven-section ASIR	LD-MBIR	<i>p</i> -Value
DLP (mGy·cm)	$5.89 \pm 1.24$	$5.04 \pm 0.52$	0.01
ED (mSv)	$0.10 \pm 0.02$	$0.08 \pm 0.01$	0.02
CTDIvol (mGy)	$46.9 \pm 9.78$	$0.017 \pm 0.01$	<0.0001

Comparison of dose measurements between seven-section and LD-MBIR protocols. Data are expressed as mean  $\pm$  SD.

LD, low dose; ASIR, adaptive statistical iterative reconstruction; MBIR, model based iterative reconstruction; DLP, dose–length product; ED, effective dose; CTDIvol, volume computed tomography dose index.

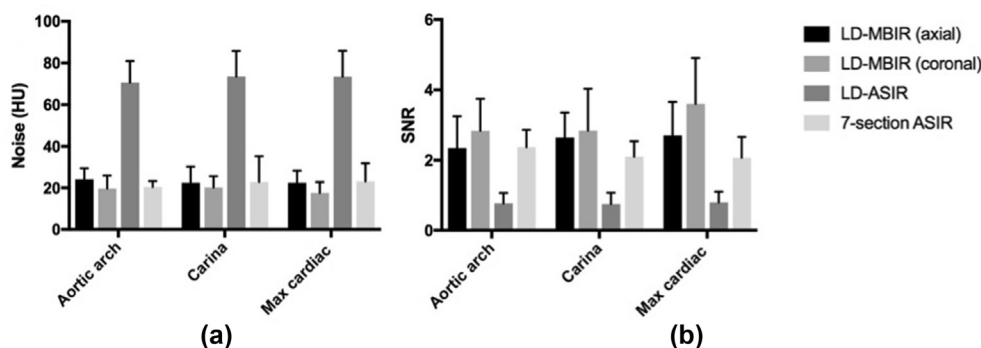


**Figure 4** Charts depicting (a) mean image noise and (b) SNR for LD-MBIR, LD-ASIR, and seven-section ASIR protocols at each of the three levels assessed. Data are plotted as mean and standard deviation as indicated by whiskers. LD-MBIR and seven-section ASIR images had significantly lower levels of image noise than LD-ASIR images. All other comparisons were non-significant. Max cardiac, maximum cardiac diameter; HU, Hounsfield units.

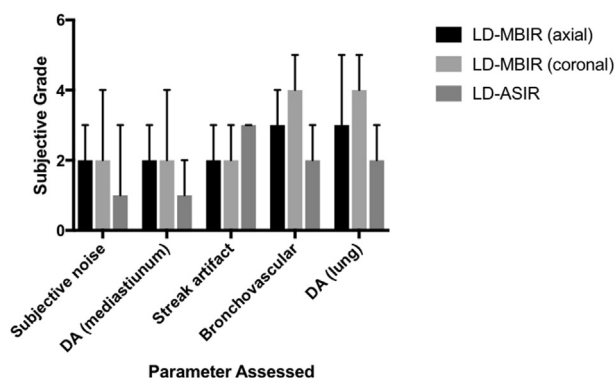


**Figure 5** Comparison of subjective image quality parameters between axial and coronal LD-MBIR and LD-ASIR datasets. Data are plotted as median and range. DA, diagnostic acceptability; bronchovascular, depiction of bronchovascular structures within 2 cm of the pleural margin.

consistent lung abnormality identified at low dose CT. All patients had bronchiectasis and it was rated as mild, moderate and severe in 22% ( $n=4$ ), 26% ( $n=5$ ), and 52% ( $n=10$ ) at 12 months, respectively, and as mild, moderate, and severe in 47.4% ( $n=9$ ), 10.5% ( $n=2$ ), and 42.1% ( $n=8$ ) at 24 months, respectively. Overall, mean severity of bronchiectasis was significantly improved at the 24-month scan (Table 2).

### Clinical course

Table 3 demonstrates change in mean BMI, FEV<sub>1</sub>, and forced vital capacity (FVC) over the study period. BMI increased significantly compared with baseline after 12 months of treatment. FEV<sub>1</sub> and FVC increased significantly compared with baseline at 12 and 24 months of treatment. No significant difference was observed for any of the measures between 12 and 24 months.

## Discussion

In recent years, there has been a sixfold increase in the use of CT in CF to monitor pulmonary disease progression and complications.<sup>21</sup> It is estimated that patients with CF will

undergo an average of 3.2 chest CT examinations during their lifetime resulting in increased lifetime cumulative effective dose compared with the general population.<sup>22</sup> Mean age at first CT examination in CF patients has also fallen, from 20 years for patients born before 1980 to 1.9 years for patients born after 1997.<sup>22</sup> Chest CT performed at such a young age can readily detect the earliest radiological manifestations of CF: mucus plugging. Chest CT has also been shown to be more sensitive for the detection of early increases in severity of lung disease and superior for the quantification of bronchiectasis compared with both PFTs and chest radiography. CT can thus provide valuable information regarding the presence and type of complications and estimation of CF lung disease severity, which represents vital information to inform important management decisions.

The major limitation to the use of CT to monitor pulmonary disease in patients with CF is the cumulative radiation dose incurred.<sup>21</sup> Physicians must remain cognisant of the risk of radiation-induced carcinogenesis, especially given the improving life expectancy among CF patients,<sup>23,24</sup> and the increasing use of CT to monitor pulmonary disease. It is imperative therefore to keep radiation exposure from chest CT as low as reasonably possible without compromising diagnostic performance.

In recent years, there has been a major industry and academic drive to develop and implement new dose-reduction technologies in CT. Chest CT is well suited to the development of dose-optimisation strategies with the high inherent contrast and low radiation absorption of the lungs.<sup>25</sup> Many dose-reduction strategies utilised to date have resulted in increased levels of image noise and reduced image quality, which have a negative impact on the ability of CT to detect and characterise pathology. Advanced IR algorithms have been introduced in recent years that serve to improve image quality through noise reduction and spatial resolution improvements, thus facilitating the generation of diagnostic quality images at reduced radiation doses. Hybrid IR techniques are applied at different blends with FBP to reduce image noise while preserving image quality and the familiar appearance of traditional FBP-reconstructed images. Hybrid IR systems have been well validated in chest CT achieving dose reductions in the order



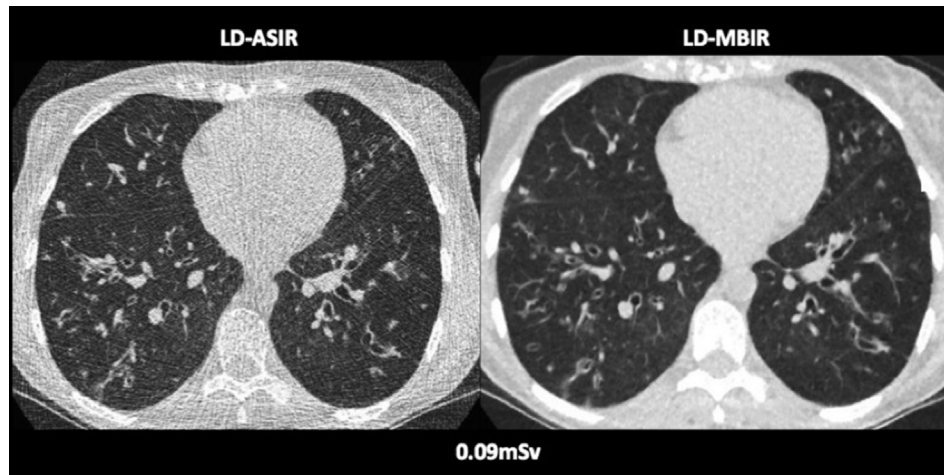


**Figure 6** Representative LD-ASIR (hybrid IR) and LD-MBIR (pure IR) axial CT images acquired in a 22-year-old woman with CF at the level of the maximum cardiac diameter illustrating the noise-reducing capabilities of MBIR (effective dose 0.09mSv). Diagnostic acceptability and depiction of bronchovascular structures with 2 cm of the pleural margin were considered acceptable for the LD-MBIR image (score of 3) and minimally acceptable (score of 2) for the LD-ASIR image.

**Table 2**

Modified Bhalla scores.

Lung abnormality	1-year	2-years
Bhalla score	11.03 ± 2.7	10.9 ± 3.99
Bronchiectasis	2.3 ± 0.82	1.9 ± 0.97 <sup>a</sup>
Peribronchial thickening	1.3 ± 0.89	0.58 ± 0.90 <sup>a</sup>
Extent of bronchiectasis	2.7 ± 0.58	2.7 ± 0.68
Extent of mucus plugging	1.5 ± 1.17	1.5 ± 0.90
Sacculations or abscesses	0.05 ± 0.23	0.74 ± 0.87 <sup>a</sup>
Generations of bronchial divisions	2.5 ± 0.90	2.3 ± 0.82
Bullae	0.26 ± 0.65	0.11 ± 0.32
Collapse or consolidation	0.37 ± 0.68	0.68 ± 0.67 <sup>a</sup>

Change in qualitative scores of disease severity, Bhalla score, between the 1-year and 2-year CT studies. Data are expressed as mean ± SD.

<sup>a</sup> Statistically significant change between the studies.

**Table 3**

Changes in clinical parameters.

	Baseline	1-year	2-years
BMI, kg/m <sup>2</sup>	21.38 ± 3.18	22.94 ± 3.63 <sup>a</sup>	22.37 ± 2.44
FEV <sub>1</sub> , % predicted	63.4 ± 17.5	74.27 ± 16.33 <sup>a</sup>	72.2 ± 17.54 <sup>a</sup>
FVC, % predicted	81.13 ± 15.16	89.87 ± 10.7 <sup>a</sup>	86.8 ± 14.07 <sup>a</sup>

Change in BMI, body mass index; FEV<sub>1</sub>, forced expiratory volume in one second; and FVC, forced vital capacity; over the study period. Data are expressed as mean ± SD.

<sup>a</sup> Statistically significant change compared to the baseline measurement.

of 46%–80% without compromising image quality.<sup>26,27</sup> Pure IR algorithms, such as MBIR used in the current study, are more computationally intense incorporating modelling of certain parameters previously omitted from the iteration process. These include a system model that addresses the nonlinear, polychromatic nature of X-ray tubes by modelling the photons in the data set, a statistical noise model that considers the focal spot and detector size, and a prior model that corrects unrealistic situations in the reconstruction process to decrease the computational time. The incorporation of system optic information enables reductions in image noise and artefacts with improvements in

spatial resolution. Pure IR has enabled even greater dose reductions than hybrid IR, with previous studies reporting the acquisition of diagnostic quality chest CT images at a dose approaching that of a PA and lateral chest radiograph (0.16 ± 0.006 mSv).<sup>19</sup> An even greater dose reduction was achieved in the present study with the protocol that enabled the acquisition of a diagnostically acceptable, full-volume, low-dose CT thorax at a dose equivalent to a PA and lateral chest radiograph (0.08 ± 0.01 mSv). Performance of hybrid IR at this dose level was suboptimal with LD-ASIR images having significantly higher levels of image noise and inferior qualitative scores than LD-MBIR images.

Initial efforts at Cork Cystic Fibrosis Centre to optimise dose from chest CT in patients with CF involved the development of a non-contiguous thin-section protocol performed at a mean effective dose of 0.1 ± 0.05 mSv in paediatric patients.<sup>7</sup> Although excellent correlation was observed between disease severity scores and chest radiography scores by O'Connor *et al.*, limiting the number of sections to reduce dose may potentially impact accuracy of assessment of true disease severity and may result in focal complications, such as mucus plugging, bronchiectasis, small areas of consolidation, or lung abscess being missed or misclassified. The current full-volume protocol enables complete evaluation of the entire lung parenchyma, mediastinum and pleural space and facilitates more reliable calculation of CT disease severity scores. In the authors' experience, this full-volume protocol is much more suitable for monitoring disease progression and guiding treatment strategies. Another major advantage is the ability to perform high-quality 3D reconstructions. Coronal reconstructions, in particular, are extremely useful in assessing disease severity and location of parenchymal and airway complications (including subtle mucus plugging, tree-in-bud opacities, and small foci of ground-glass opacification) which may herald early signs of disease progression in CF. The additional information provided by the current low-



dose CT protocol at a dose equivalent to chest radiography has been appreciated by respiratory physician colleagues and has led to LDCT (LDMBIR protocol) replacing chest radiography in CF patients for most clinical indications.

There are several limitations to the present study. A concurrent conventional dose CT scan was not performed as a reference standard; however, an additional conventional dose study was not ethically justifiable as the aim was to develop a low-dose protocol to replace chest radiography for the purpose of routine pulmonary disease assessment, and as all patients were clinically stable, no indication existed to perform a conventional dose study. Comparison of disease severity scores may not be entirely comparable, as the seven-section protocol may have led to clinically important disease being missed. In addition, expiratory phase imaging was omitted from the LD-MBIR protocol in the interests of reducing dose as much as was possible. Furthermore, the present patient cohort was small, which limits the strength of the conclusions drawn. Imaging of the mediastinum and upper abdomen was suboptimal with both protocols; however, assessment of the mediastinum is of less concern in patients with CF where evaluation of pulmonary disease is the primary intention. This is therefore an acceptable limitation, given the substantial reduction in radiation dose achieved.

The findings of the present study strengthen the case for the use of low-dose CT in patients with CF with some experts suggesting that surveillance CT should be performed biannually.<sup>28</sup> The present low-dose protocol could also potentially have a role in screening for non-CF bronchiectasis. Low-dose CT in this setting may detect mild bronchiectasis and prevent patients with early bronchiectasis and a normal chest radiograph being misdiagnosed as having asthma.<sup>29</sup> Thus, in the assessment of non-CF patients presenting with suspected bronchiectasis, consideration should be given to the replacement of chest radiograph with low-dose chest CT reconstructed with pure IR.

In conclusion, the use of MBIR with a volumetric low-dose protocol enabled the acquisition of diagnostic quality chest CT images in CF patients at a dose equivalent to that of a PA and lateral chest radiograph.

## Conflict of interest

The authors declare no conflict of interest.

## Acknowledgements

The authors are grateful to the following, for their insights and contributions: Dr Maria Twomey, Dr Karl James, Ms Mairead McCarthy, Dr Desmond Murphy, Prof. Fergus Shanahan, Prof. Joe A Eustace, Prof. Mark F McEntee. This research was supported by Science Foundation Ireland through a centre research grant to APC Microbiome, UCC, Cork, Ireland.

## References

1. Wood BP. Cystic fibrosis: 1997. *Radiology* 1997;**204**:1–10.

2. Weiser G, Kerem E. Early intervention in CF: how to monitor the effect. *Pediatr Pulmonol* 2007;**42**:1002–7.
3. Que C, Cullinan P, Geddes D. Improving rate of decline of FEV1 in young adults with cystic fibrosis. *Thorax* 2006;**61**:155–7.
4. de Jong PA, Lindblad A, Rubin L, et al. Progression of lung disease on computed tomography and pulmonary function tests in children and adults with cystic fibrosis. *Thorax* 2006;**61**:80–5.
5. Judge EP, Dodd JD, Masterson JB, et al. Pulmonary abnormalities on high-resolution CT demonstrate more rapid decline than FEV1 in adults with cystic fibrosis. *Chest* 2006;**130**:1424–32.
6. Li J, Udayasankar UK, Toth TL, et al. Automatic patient centering for MDCT: effect on radiation dose. *AJR Am J Roentgenol* 2007;**188**:547–52.
7. O'Connor OJ, Vandeleur M, McGarrigle AM, et al. Development of low-dose protocols for thin-section CT assessment of cystic fibrosis in pediatric patients. *Radiology* 2010;**257**:820–9.
8. Ronan NJ, Einarsson GG, Twomey M, et al. CORK study in cystic fibrosis: sustained improvements in ultra-low-dose chest CT scores after CFTR modulation with ivacaftor. *Chest* 2018;**153**:395–403.
9. Ramsey BW, Davies J, McElvaney NG, et al. A CFTR potentiator in patients with cystic fibrosis and the G551D mutation. *N Engl J Med* 2011;**365**:1663–72.
10. Davies JC, Wainwright CE, Canny GJ, et al. Efficacy and safety of ivacaftor in patients aged 6 to 11 years with cystic fibrosis with a G551D mutation. *Am J Respir Crit Care Med* 2013;**187**:1219–25.
11. Barry PJ, Plant BJ, Nair A, et al. Effects of ivacaftor in patients with cystic fibrosis who carry the G551D mutation and have severe lung disease. *CHEST J* 2014;**146**:152–8.
12. Scotet V, Barton DE, Watson JB, et al. Comparison of the CFTR mutation spectrum in three cohorts of patients of Celtic origin from Brittany (France) and Ireland. *Hum Mutat* 2003;**22**:105.
13. Cystic Fibrosis Foundation. *Patient registry. Annual data report*. 2015. Bethesda, MD. Available at: <https://www.cff.org/our-research/cf-patient-registry/2015-patient-registry-annual-data-report.pdf>. [Accessed 8 January 2021].
14. Bobadilla JL, Macek Jr M, Fine JP, et al. Cystic fibrosis: a worldwide analysis of CFTR mutations—correlation with incidence data and application to screening. *Hum Mutat* 2002;**19**(6):575–606.
15. De Boeck K, Zolin A, Cuppens H, et al. The relative frequency of CFTR mutation classes in European patients with cystic fibrosis. *J Cyst Fibros* 2014;**13**(4):403–9.
16. Qi L, Li Y, Tang L, et al. Evaluation of dose reduction and image quality in chest CT using adaptive statistical iterative reconstruction with the same group of patients. *Br J Radiol* 2012;**85**:e906–11.
17. Prakash P, Kalra MK, Ackman JB, et al. Diffuse lung disease: CT of the chest with adaptive statistical iterative reconstruction technique. *Radiology* 2010;**256**:261–9.
18. Lucas L, Geyer U, Joseph Schoepf, et al. State of the art: iterative CT reconstruction techniques. *Radiology* 2015;**276**(2):339–57.
19. Neroladaki A, Botsikas D, Boudabbous S, et al. Computed tomography of the chest with model-based iterative reconstruction using a radiation exposure similar to chest X-ray examination: preliminary observations. *Eur Radiol* 2013;**23**:360–6.
20. Bhalla M, Turcios N, Aponte V, et al. Cystic fibrosis: scoring system with thin-section CT. *Radiology* 1991;**179**:783–8.
21. O'Connell OJ, McWilliams S, McGarrigle A, et al. Radiologic imaging in cystic fibrosis: cumulative effective dose and changing trends over 2 decades. *Chest* 2012;**141**:1575–83.
22. Donadieu J, Roudier C, Saguinthaah M, et al. Estimation of the radiation dose from thoracic CT scans in a cystic fibrosis population. *Chest* 2007;**132**:1233–8.
23. Maisonneuve P, Marshall BC, Knapp EA, et al. Cancer risk in cystic fibrosis: a 20-year nationwide study from the United States. *J Natl Cancer Inst* 2012;**105**:122–9.
24. MacKenzie T, Gifford AH, Sabadosa KA, et al. Longevity of patients with cystic fibrosis in 2000 to 2010 and beyond: survival analysis of the Cystic Fibrosis Foundation Patient Registry. Lifetime of patients with cystic fibrosis in 2000 to 2010 and beyond. *Ann Intern Med* 2014;**161**:233–41.
25. Itoh S, Ikeda M, Arahata S, et al. Lung cancer screening: minimum tube current required for helical CT. *Radiology* 2000;**215**:175–83.
26. Laqmani A, Buhk J, Henes F, et al. Impact of a 4th generation iterative reconstruction technique on image quality in low-dose computed

- tomography of the chest in immunocompromised patients. *Rofo* 2013;**185**:749–57.
27. Kalra MK, Woisetschläger M, Dahlström N, et al. Sinogram-affirmed iterative reconstruction of low-dose chest CT: effect on image quality and radiation dose. *AJR Am J Roentgenol* 2013;**201**:W235–44.
28. Loeve M, Lequin MH, de Bruijne M, et al. Cystic fibrosis: are volumetric ultra-low-dose expiratory CT scans sufficient for monitoring related lung disease? *Radiology* 2009;**253**:223–9.
29. Li A, Sonnappa S, Lex C, et al. Non-CF bronchiectasis: does knowing the aetiology lead to changes in management? *Eur Resp J* 2005;**26**:8–14.